A Bioinspired Approach to Torque Control in an Insect-sized Flapping-wing Robot

Zhi Ern Teoh and Robert J. Wood

***Abstract*— A flapping-wing micro air vehicle was built that mimics the control strategy utilized by fruit flies which indirectly modulate wing angle of attack to generate yaw torques. This prototype could also generate roll torques by oscillating the wing hinge at the flapping frequency with an appropriate phase. The roll, yaw and pitch torque generation capability was characterized using a custom single-axis torque sensor. The vehicle could produce torques with magnitudes of 0.8μNm, 1μNm and 0.8μNm of roll, yaw and pitch torque respectively. Based off Sthe known inertial properties of the robot, we estimate that it is capable of achieving turning performances comparable to fruit flies.**

I. Introduction

The insect world presents some remarkable feats of flight maneuvers that serve as motivations for engineers striving to create bioinspired flying robots. Just to name a few examples, bees forage in highly dynamic and cluttered environments, dragonflies fly backwards and hoverflies perform 90° saccades in only a few wing beats. Such impressive flight capabilities have inspired researchers and engineers to elucidate key principles behind insect flight - not only to understand how insects fly but also to build increasingly smaller and more maneuverable micro air vehicles. Several important fluid mechanics phenomena are crucial for insect flight: a stable leading edge vortex along the wing, rotational lift during the transition from upstroke to downstroke and wake capture which enables the wings to recover some energy from the wake of the previous half wing stroke [1], [2]. By designing robots that utilize these fluid phenomena [3], [4], [5], one goal is to build vehicles capable of operating in hazardous and cluttered environments where maneuverability is paramount.

The Harvard Microrobotic Fly (HMF), a flapping-wing micro air vehicle (FWMAV) having a wing span of 3cm and weighing 60mg, was the first vehicle of its size to lift its own weight up two vertical guide wires. The key to this flight was the use of passive wing rotation - where the compliance of a flexure hinge interacts with the wing inertia and aerodynamic loading on the wing to produce a desired angle of attack. This removed the need to actively control the wings' angle of attack, reducing the weight of the vehicle which enabled take-off [6]. The HMF, however, could not control itself when the guide wires were removed. A single actuator driving both wings could not generate control torques to maintain its upright position. Work by Teoh [7] sought to control the FWMAV by altering the body of the HMF by adding passive aerodynamic dampers that stabilized the FWMAV about its roll and pitch axes. Though the FWMAV was able to maintain upright stability, hover was unattainable due to uncontrollable rotations along the FWMAV's yaw axis.

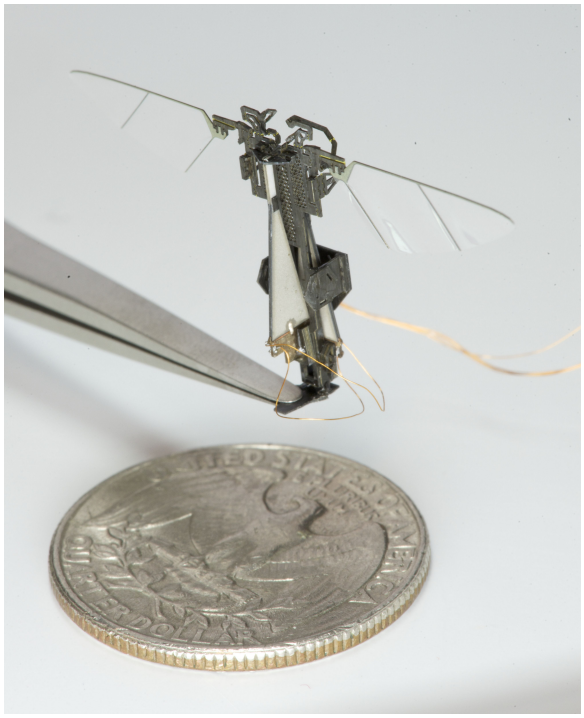

Fig. 1. A bioinspired FWMAV employing a differential mechanism enabling indirect control over the wings' angle of attack

In order to produce control torques about all three body axes, additional actuated degrees of freedom are needed. Inspired by neopteran insects that have two distinct sets of muscles (power muscles which drive the wings at the resonant frequency of the wing/thorax system and smaller muscles at the wing base that subtly alter wing kinematics), Finio [8] designed a FWMAV that had a single power actuator driving two wings and two smaller control actuators at the base of the wing transmissions which altered the transmission ratios of the left and right wing. This

This work was partially supported by the National Science Foundation (award numbers CCF-0926148 and CMMI-0746638) and the Wyss Institute for Biologically Inspired Engineering. Any opinions, findings, and conclusions or recommendations expressed in this material are those of the authors and do not necessarily reflect the views of the National Science Foundation.

The authors are with the School of Engineering and Applied Sciences, Harvard University, Cambridge MA 02138 USA and the Wyss Institute for Biologically Inspired Engineering, Harvard University, Boston, MA 02115, USA (E-mail: zhiernteoh@seas.harvard.edu and rjwood@eecs.harvard.edu)

enabled the FWMAV to control its left and right wing stroke amplitude producing appreciable control torques. Another approach taken by Ma gave each wing its own actuator [9]. This proved to be successful in producing sufficient control torques, resulting in the first controlled hover of an insect-scale FWMAV [10]. In both cases, angle of attack is modulated through changes in the wing stroke amplitude. Roll torque is generated by flapping one wing at a relatively larger amplitude than the other and pitch torque is produced by biasing the mean of the stroke amplitude. Yaw torque is generated by breaking up the wing stroke into two portions - a slow stroke in one direction and a fast stroke in the other - while maintaining a constant wingbeat period [11]. The idea behind this maneuver is to use asymmetric drag profiles caused by differences in the wing velocity during the upstroke and downstroke to create a net yaw torque. The fast portion of the wing stroke requires adding a second harmonic component to the actuation commands of the FWMAV. Ma reports in [9] that the wing stroke velocity profile tended to remain nearly symmetrical, resisting efforts to develop an asymmetry which hindered yaw torque production.

For an alternative mechanism, we look to nature for inspiration. Data gleaned from studying the free-flight kinematics of the fruit fly (*D. melanoaster*) suggests that fruit flies employ a simple bias of their wing hinge to create asymmetric drag profiles during upstroke and downstroke, resulting in a yaw torque [12]. This idea is elegant in principle, however, its mechanical instantiation is complex relative to the previous examples [13]. Fortunately, recent developments in the Smart Composite Microstructures (SCM) process [14], [15], [16] have enabled us to explore devices with such a level of mechanical complexity. Looking at just the right side of the FWMAV (figure 2), two pairs of planar four-bar linkages convert quasi-linear control and power inputs into angular motions, θ_R and ϕ_R respectively, a spherical four-bar linkage rotates the axis of the angular motion θ_R by 90° creating an angular control input ς_R and a spherical five-bar linkage which combines the angular control and power inputs (ς_R and ϕ_R respectively) by mapping them onto the wing hinge. Further refinement of the FWMAV presented in [13] has enabled us to begin characterizing its torque generation capability allowing us to move one step closer towards building a flight-weight version. One of the key questions in developing a flight-weight version is the sizing of the control actuator such that sufficient torques are generated for control, while minimizing weight of the control infrastructure. This is one of the motivations for the experimental characterization presented in this paper.

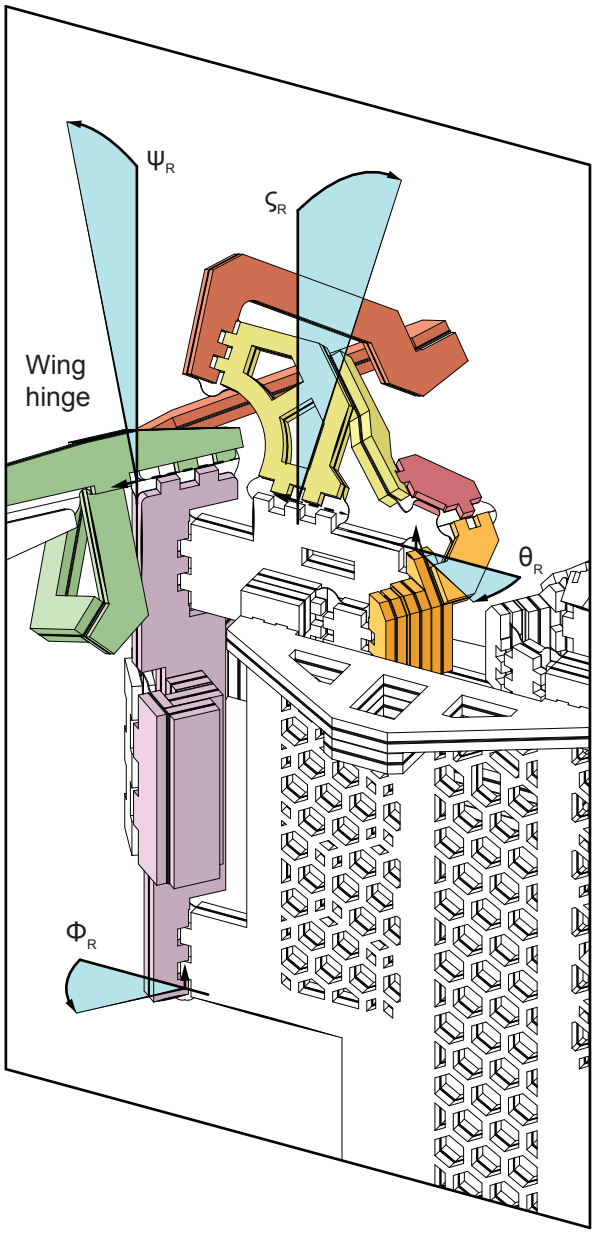

Fig. 2. Right sided close-up of the FWMAV. Spherical four-bar linkage consists of orange, magenta and yellow components. Spherical five-bar linkage comprises the purple, green (wing hinge), red and yellow parts.

II. Indirect modulation of the wing's angle of attack: A Review

The hinge that connects the wing to the body of the FWMAV is modeled as a torsional spring that generates a restorative torque in response to deformations from inertial and aerodynamic forces. By changing the rest angle of the spring from its neutral point, the amount of restorative torque exerted by the spring changes. This in turn affects the wing pitch angle which gives rise to different angles of attack during the upstroke and downstroke [12]. Since aerodynamic forces are functions of the angle of attack, control torques generated by aerodynamic forces can be manipulated by modulating the angle of attack.

In this FWMAV, a single power actuator is used to drive both wings (fig. 3D). To save weight, a single control actuator is used to cause a bilaterally opposite change in the left and right spring rest angle (ψ_L and ψ_R) as shown in figure 3C (i.e. if the right is biased +10 deg the left is biased -10 deg) [13]. To generate pitch torques, the power actuator is biased to shift the mean stroke angle further towards the upstroke or downstroke [17]. Inspired by the fruit flies, yaw torque is produced by a fixed bias of the spring rest angle. This causes

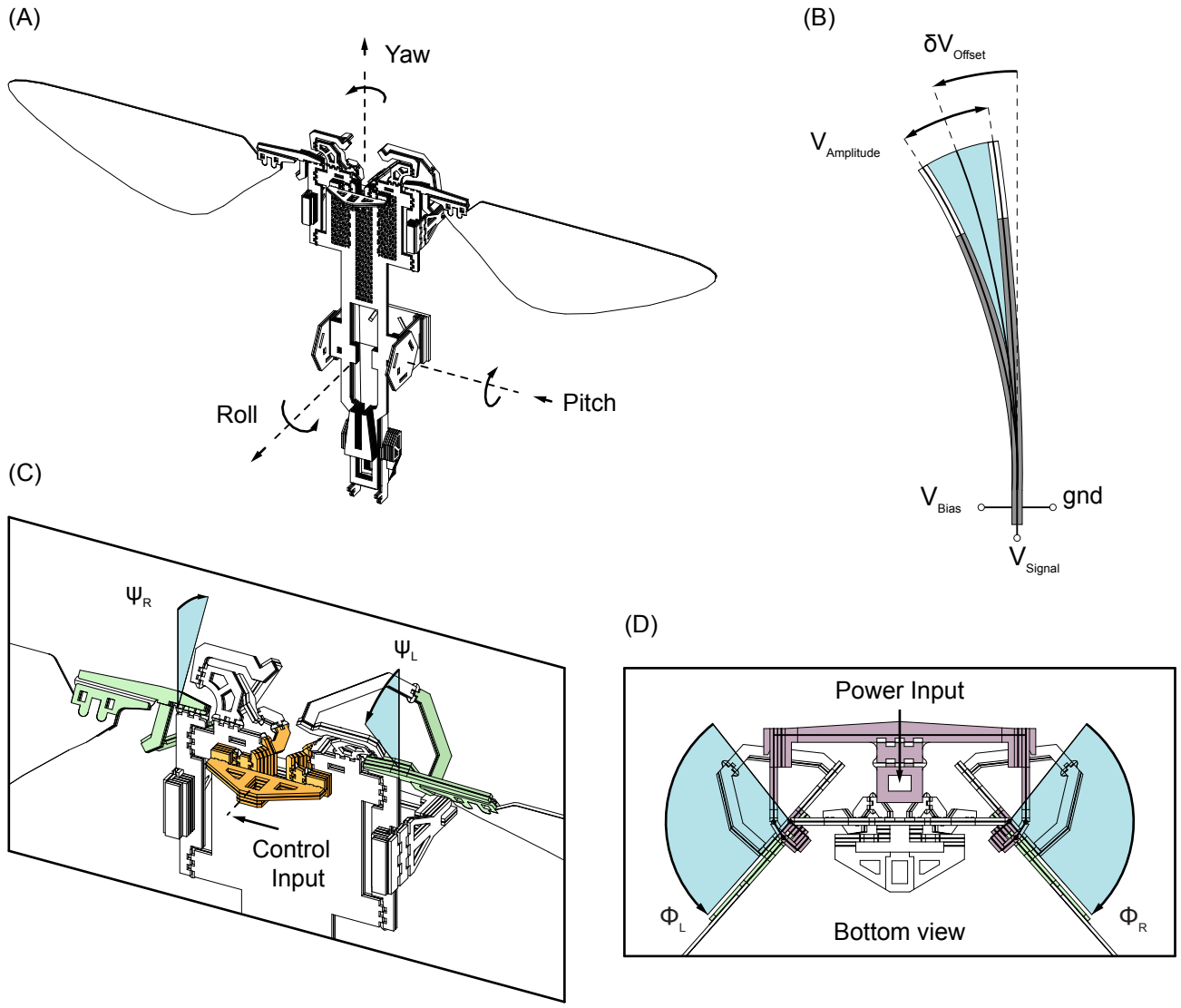

Fig. 3. (A) Convention used to define the three axes of the FWMAV. (B) Electrical signal input to an actuator and the corresponding actuator tip output. (C) Control actuator input biases the left and right wing hinge (green) in a bilaterally opposite way. (D) Power actuator input changes the magnitude of the wing stroke angle amplitude (ϕ_L and ϕ_R) and the location of the mean wing stroke angle.

the upstroke and the downstroke of the wing to have two distinct angles of attack, generating a net drag asymmetry between the upstroke and downstroke [12]. Consequently, the net drag generates a torque that causes the vehicle to yaw. Taking this concept one step further, by oscillating the control actuator at the flapping frequency, either in phase or out of phase with the power actuator, roll torques are generated [13].

In order to design a FWMAV that can hover using this concept of indirect manipulation of the angle of attack, the control torques (roll, yaw and pitch) must be characterized. Knowing how much torque can be produced for each axis, along with potential coupling of torques would provide useful insights for designing control laws and would inform appropriate sizing of the control actuator to minimize weight while providing sufficient control torques for hovering flight.

III. Results and Discussion

The vehicle is mounted onto a custom single-axis torque sensor consisting of a cross shaped sensing beam that is designed to be sensitive to a torque applied along the long axis of the beam but insensitive to all other torques and forces (figure 4). A capacitive sensor measures the change in displacement of a target plate on the sensing beam by sensing changes in voltages (sampled at 5 KHz) as the plate moves up and down in response to a torque twisting the beam [18]. To measure torques about the roll, yaw and pitch axes of the vehicle, the vehicle has to be reoriented to align the torque sensing axis of the sensor to the desired axis of the vehicle. To minimize the effect of lift on the sensor measurements in the roll and pitch measuring orientations, the vehicle is mounted in such a way that lift is orthogonal to the displacement of the target plate (figure 4). For the pitch measuring orientation, we assume that aerodynamic drag due to the flapping wings is zero-averaged and has minimal effect

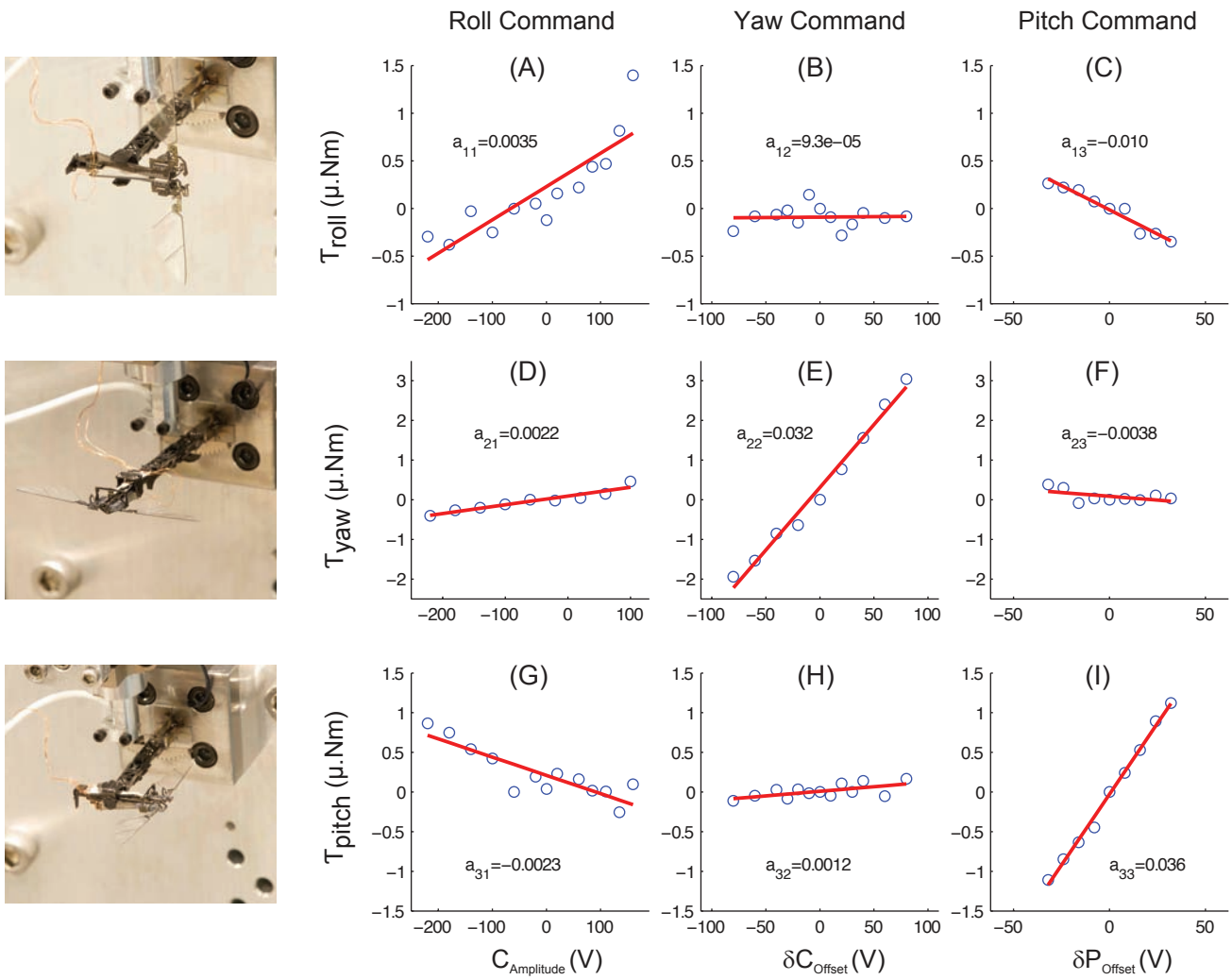

Fig. 5. Measured torque along the FWMAV's body axis as a function of roll, yaw or pitch control commands. For each data set, a least squares fit was applied as is shown in red. The gradient of each line is labelled a_{ij} where i refers to the row number and j the column number.

on the displacement of the target plate.

For the purpose of torque characterization, the control actuator is identical to the power actuator. These piezoelectric bimorph actuators [19] are made by sandwiching a carbon fiber layer between two Lead Zirconate Titanate (PZT) plates (Piezo Systems Inc.). A bias voltage, V_{Bias}, of $300V$ is applied to the top plate and $0V$ is applied to the bottom plate (order depends on poling direction of the PZT plates). The control signal (replacing V with either P or C refers to the power or control actuator, respectively)

$$V_{Signal} = \frac{V_{Amplitude}}{2}(sin2\pi f_{Op}t) + \frac{V_{Bias}}{2} + \delta V_{Offset}$$

is applied at the carbon fiber layer of the power and control actuators. Increasing $P_{Amplitude}$ increases the power actuator's tip to tip displacement which increases the vehicle's flapping amplitude. A change in δP_{Offset} generates a pitch torque by shifting the mean displacement of the power actuator which also shifts the mean of the wing stroke amplitude (figure 3B). To produce a yaw torque, a change in δC_{Offset} of the control actuator causes a bilaterally opposite change in the rest angle of the left and right wing hinges. To create roll torques, $C_{Amplitude}$, in combination with input from the power actuator, is increased to increase the magnitude of the oscillating spring rest angle (figure 3C). The operating frequency, f_{Op}, of the vehicle was set to its resonant frequency of 100 Hz and $P_{Amplitude}$ was set to a moderate $225V$ (this was done to prolong the life time of the FWMAV) which produced a peak-to-peak stroke amplitude of approximately 70°. Each experiment lasted one second and torques were averaged from the resulting 100 flapping periods for various combinations of power and control actuator inputs. Roll commands ($C_{Amplitude}$) were varied from -220V to 160V, yaw commands (δC_{Offset}) were varied between -80V to 80V while pitch commands (δP_{Offset}) were swept from -32V to 32V.

The torque sensor was calibrated by hanging a $205mg$ weight at $1mm$ intervals on notches along the sensing beam (figure 4). Due to drifts in the voltage signal, we take the difference in voltage readings before and after a weight is added. This creates a calibration curve from a set of known torques with a corresponding set of voltage differences.

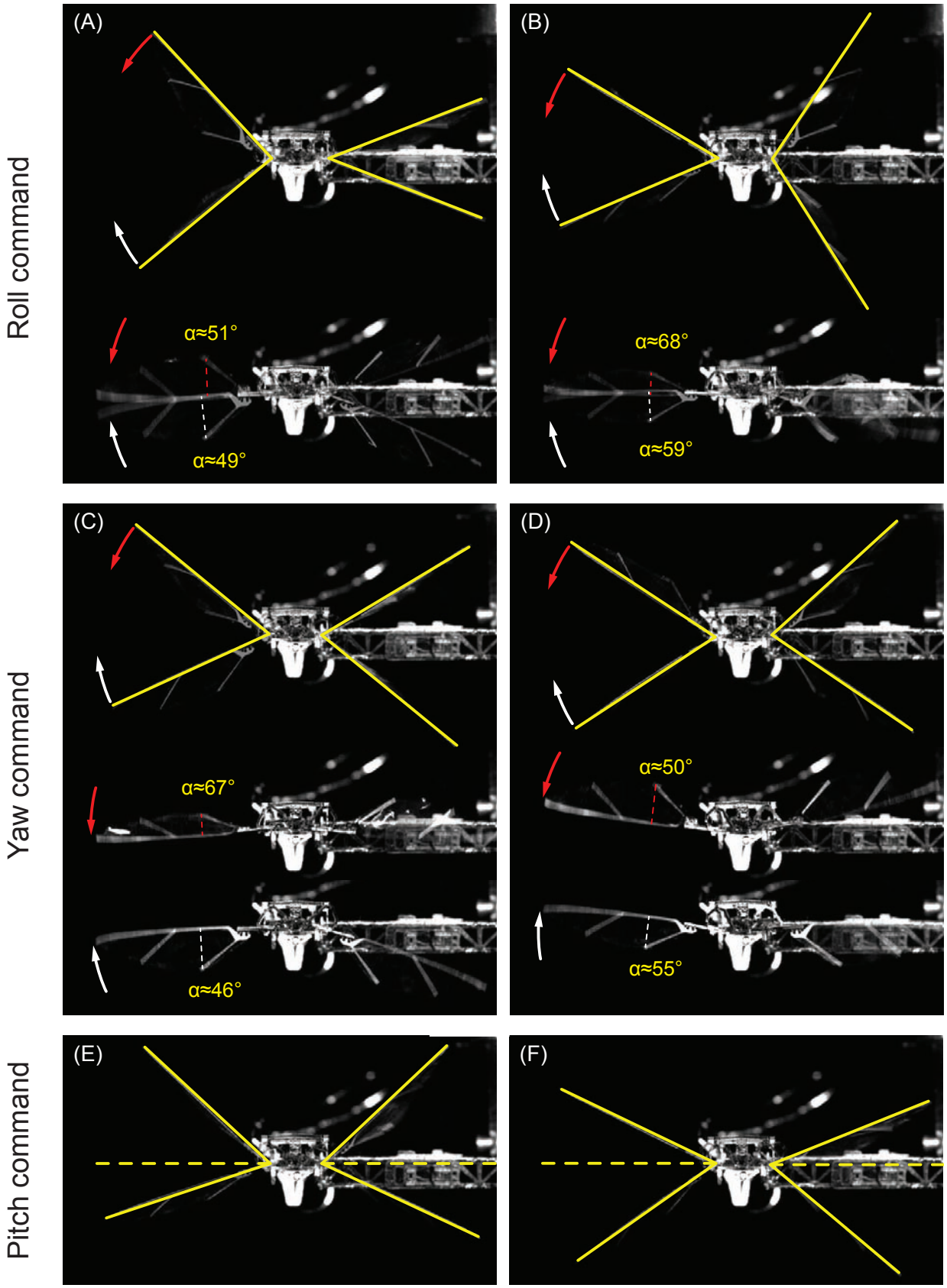

Fig. 6. Still frames from high speed video taken at 3000 fps. From left to right: (A-B) Roll commands were $C_{Amplitude}$ = -220V and 160V. (C-D) Yaw commands were δC_{Offset} = -80V and 80V. (C) Pitch commands were δP_{Offset} = -32V and 32V

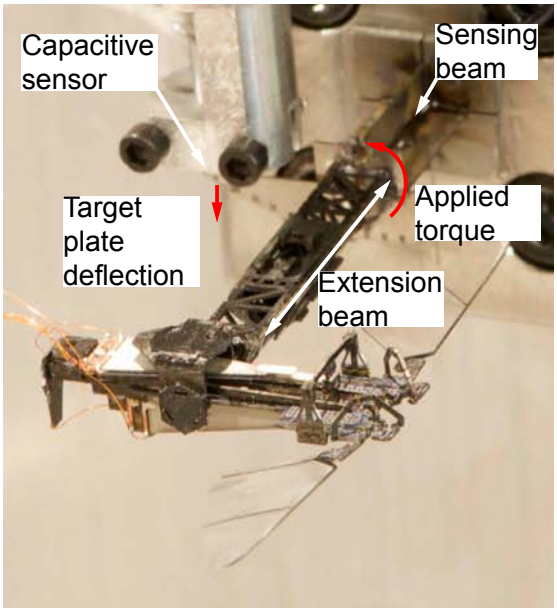

Fig. 4. The FWMAV mounted on a custom single axis torque sensor. Here the vehicle is placed in the pitch torque measuring orientation.

When the FWMAV is given a control signal, we measure the voltage difference before and after the torque command was issued and use the calibration curve to back out the torque generated by the FWMAV.

Figure 5 shows the measured torques about the roll, yaw and pitch axes. Each row presents torque measurements about a particular axis (roll, yaw or pitch) while each column indicates what type of torque command (roll, yaw or pitch) is issued. Roll, yaw and pitch torques showed positive correlations with their respective commands with roll torques exhibiting a positive bias at the extreme of the positive roll torque command at an amplitude $C_{Amplitude} = 160V$. At a smaller $C_{Amplitude}$ of $160V$, the magnitude of the roll torque was expected to be smaller than the magnitude of roll torque at $C_{Amplitude}$ of $-220V$. In figure 6B the difference in stroke amplitude of the left wing over the right wing was 58° while the difference in the stroke amplitude of the right wing over the left wing in figure 6A was 45°. This suggests that the sharp increase in roll torque at $C_{Amplitude} = 160V$ was due to the larger difference in stroke amplitude which caused the positive torque bias. This bias could be due to a combination of manufacturing misalignment and an inherent deflection bias of the control actuator.

The right wing's angle of attack at the mid-stroke was estimated by measuring the wing chord projected on the image plane (highlighted by dashed lines in figure 6A) and the known chord length. In figure 6A, the angle of attack was 51° on the downstroke and 49° on the upstroke while in figure 6B the angle of attack was 68° on the downstroke and 59° on the upstroke. This increase in the angle of attack highlights the effect of how the oscillating rest angle of the right wing can indirectly control the angle of attack, enabling the vehicle to transition from negative to positive roll torques.

The effect of biasing the rest angle on the angle of attack during the upstroke and downstroke of the right wing is highlighted in figure 6C and D. In figure 6C, the difference between the angle of attack on the downstroke and upstroke was +21°. The downstroke experienced more drag than the upstroke because more of the wing was exposed to the incoming flow of air, creating a net thrust that produced a negative yaw torque. When biasing the spring rest angle in the opposite direction, the difference between the angle of attack on the downstroke and on the upstroke was -5° which created a positive yaw torque (figure 6D).

Torque data for off-axis commands showed a relatively flat response to on-axis commands except for coupling observed in the roll torque - pitch command and pitch torque - roll command experiments (figure 5C and G). Roll torque - pitch command data exhibited a negative correlation between roll torque and pitch command while pitch torque - roll command data was largely flat in the direction of positive roll commands but negatively correlated in the direction of negative roll torque commands.

Assuming the elements a_{ij} are constant and independent from the actuator inputs, the gradients from figure 5 are assembled into a matrix A, establishing a relationship between torque produced and control inputs (the offsets of the least squares fit are ignored because of the inherent torque biases in the FWMAV due to the imperfect manufacturing and mounting of the vehicle to the sensor beam),

$$\begin{bmatrix} \tau_{roll} \\ \tau_{yaw} \\ \tau_{pitch} \end{bmatrix} = \begin{bmatrix} a_{11} & a_{12} & a_{13} \\ a_{21} & a_{22} & a_{23} \\ a_{31} & a_{32} & a_{33} \end{bmatrix} \begin{bmatrix} C_{Amplitude} \\ \delta C_{Offset} \\ \delta P_{Offset} \end{bmatrix} \quad (1)$$

$$\vec{\tau} = A\vec{x}. \quad (2)$$

$$\vec{\tau} = \begin{bmatrix} 0.0035 & 9.3e-05 & 0.010 \\ 0.0022 & 0.032 & -0.0038 \\ -0.0023 & 0.0012 & 0.036 \end{bmatrix} \vec{x} \quad (3)$$

From the values given in equation 3, the rank of A is 3 and its condition number is 14. This implies that if the FWMAV requires a desired torque vector, $\vec{\tau}_{des}$, to remain upright in hover, we could in principle find a set of desired control inputs by inverting A

$$\vec{x}_{des} = A^{-1}\vec{\tau}_{des} \quad (4)$$

Fruit flies can execute a 45° yaw turn in $22ms$ [12]. Using this as a benchmark for this FWMAV, a yaw torque of $\pm 1\mu Nm$ together with its yaw axis moment of inertia estimate of $0.35gmm^2$, would execute a similar yaw maneuver in $22ms$. From equation 4,

$$\vec{x}_{des} = A^{-1} \begin{bmatrix} 0 \\ \pm 1 \\ 0 \end{bmatrix}$$

$$\vec{x}_{des} = \begin{bmatrix} \mp 4 \\ \pm 32 \\ \mp 1 \end{bmatrix}$$

sets a yaw command (δC_{Offset}) range of -32V to 32V. This implicitly sets a bound on how high $C_{Amplitude}$ can

go because $min(C_{Signal}) \geq 0$ and $max(C_{Signal}) \leq V_{bias}$. If these limits are exceeded the control actuator would start to de-pole. As a result, the range of $C_{Amplitude}$ is set to -236V to 236V and the expected roll torque achievable is $\pm 0.8 \mu Nm$. Again comparing to fruit flies which were observed to perform a roll turn of 45° in less than $50ms$ [20], a roll torque of $0.8 \mu Nm$ with its roll axis moment of inertia estimate of $2.14 gmm^2$ would roll 45° in $65ms$. To generate similar torques in the pitch axis of $\pm 0.8 \mu Nm$, the pitch command (δP_{Offset}) range is set to -$23V$ and $23V$ which leaves a $max(P_{Amplitude})$ of $254V$.

The use of equation 4 for flight control should be used conservatively and limited to only small desired torque outputs. The system matrix A was assumed constant and independent from the control inputs $\vec{x}$. In reality, the elements of A, are most likely a function of the control and power actuator inputs $C_{Amplitude}$, δC_{Offset}, $P_{Amplitude}$ and δP_{Offset}. If more aggressive torque outputs are required for hover, the relationship between torques and control inputs need to be probed at a deeper level involving combinations of multiple control inputs.

IV. Conclusions and Future Work

The results show that indirect modulation of the wings' angle of attack through direct control of the wing hinge rest angle is a viable means of creating torques to control an insect-scale FWMAV. A more in-depth study of dynamic coupling must be investigated. In this series of experiments, only a single torque command was issued during a trial. Future experiments involving a combination of three torque commands are essential because all three torques are most likely needed to maintain the stability of the FWMAV in hover. By using a multi-axis torque sensor, adverse coupling of the torques could be characterized a priori to aid in the design of a flight controller.

References

[1] C.P. Ellington, C. Van Den Berg, A.P. Willmott, and Adrian LR Thomas. Leading-edge vortices in insect flight. *Nature*, 384:626–630, 1996.

[2] M.H. Dickinson, F. Lehmann, and S.P. Sane. Wing rotation and the aerodynamic basis of insect flight. *Science*, 204:1954–1960, 1999.

[3] De Croon, De Clercq, R Ruijsink, B Remes, and C De Wagter. Design, aerodynamics, and vision-based control of the delfly. *International Journal of Micro Air Vehicles*, 1(2):71–97, 2009.

[4] F. van Breugel, W. Regan, and H. Lipson. From insects to machines. *IEEE Robotics & Automation Magazine*, 15(4):68–74, 2008.

[5] M. Keennon, K. Klingebiel, H. Won, and A. Andriukov. Development of the nano hummingbird: A tailless flapping wing micro air vehicle. In *AIAA Aerospace Sciences Meeting*, 2012.

[6] R. J. Wood. Liftoff of a 60mg flapping-wing mav. In *Proc. IEEE/RSJ Int. Conf. Intelligent Robots and Systems IROS 2007*, pages 1889–1894, 2007.

[7] Z.E. Teoh, S.B. Fuller, P. Chirarattananon, NO Prez-Arancibia, J.D. Greenberg, and R.J. Wood. A hovering flapping-wing microrobot with altitude control and passive upright stability. In *Intelligent Robots and Systems (IROS), 2012 IEEE/RSJ International Conference on*, pages 3209–3216. IEEE, 2012.

[8] B.M. Finio and R.J. Wood. Open-loop roll, pitch and yaw torques for a robotic bee. In *Intelligent Robots and Systems (IROS), 2012 IEEE/RSJ International Conference on*. IEEE, 2012.

[9] K.Y. Ma, S.M. Felton, and R.J. Wood. Design, fabrication, and modeling of the split actuator microrobotic bee. In *Intelligent Robots and Systems (IROS), 2012 IEEE/RSJ International Conference on*. IEEE, 2012.

[10] K.Y Ma, P. Chirarattananon, S.B. Fuller, and R.J. Wood. Controlled flight of a biologically inspired, insect-scale robot. *Science*, 340(6132):603–607, 2013.

[11] D. Doman, M.W. Oppenheimer, and D. Sigthorsson. Dynamics and control of a minimally actuated biomimetic vehicle: Part i-aerodynamic model. In *AIAA Guidance, Navigation, and Control Conference, AIAA Paper*, volume 6160, 2009.

[12] A.J. Bergou, L. Ristroph, J. Guckenheimer, I. Cohen, and Z.J. Wang. Fruit flies modulate passive wing pitching to generate in-flight turns. *Physical review letters*, 104(14):148101, 2010.

[13] Z.E. Teoh and R.J. Wood. A flapping-wing microrobot with a differential angle-of-attack mechanism. In *Robotics and Automation (ICRA), 2013 IEEE/RSJ International Conference on*. IEEE, 2013.

[14] R.J. Wood, S. Avadhanula, R. Sahai, E. Steltz, and R.S. Fearing. Microrobot design using fiber reinforced composites. *Journal of Mechanical Design*, 130(5):052304, 2008.

[15] P.S. Sreetharan, J.P. Whitney, and R.J. Strauss M., and Wood. Monolithic fabrication of millimeter-scale machines. *Journal of Micromechanics and Microengineering*, 2012.

[16] J.P. Whitney, P.S. Sreetharan, K.Y. Ma, and R.J. Wood. Pop-up book mems. *Journal of Micromechanics and Microengineering*, 21(11):115021–115027, 2011.

[17] N.O. Pérez-Arancibia, P. Chirarattananon, B.M. Finio, and R.J. Wood. Pitch-angle feedback control of a biologically inspired flapping-wing microrobot. In *Robotics and Biomimetics (ROBIO), 2011 IEEE International Conference on*, pages 1495–1502. IEEE, 2011.

[18] B.M. Finio, K.C. Galloway, and R.J. Wood. An ultra-high precision, high bandwidth torque sensor for microrobotics applications. In *Intelligent Robots and Systems (IROS), 2011 IEEE/RSJ International Conference on*, pages 31–38. IEEE, 2011.

[19] R.J. Wood, E. Steltz, and R.S. Fearing. Optimal energy density piezoelectric bending actuators. *Sensors and Actuators A: Physical*, 119(2):476–488, 2005.

[20] S.N. Fry, R. Sayaman, and M.H. Dickinson. The aerodynamics of free-flight maneuvers in drosophila. *Science*, 300(5618):495–498, 2003.